

EQCM Study of the Adsorption of Polyethyleneglycol With Different Molecular Weights and its Coadsorption With Cl⁻ ions on Pt in Perchloric Acid Solution

Alia Méndez, L.E. Moron, G. Orozco, R. Ortega-Borges, Y. Meas, G. Trejo *

Centro de Investigación y Desarrollo Tecnológico en Electroquímica (CIDETEQ). Parque Tecnológico Sanfandila, Pedro Escobedo, Querétaro, A.P. 064. C.P. 76703, Querétaro, México

*E-mail: gtrejo@cideteq.mx

Received: 24 September 2010 / Accepted: 15 October 2010 / Published: 1 December 2010

The adsorption of polyethyleneglycol with different molecular weights (PEG_x ; $x = 400, 3000, 8000$, or 20000), and its coadsorption with Cl^- ions, was investigated using cyclic voltammetry (CV) in conjunction with simultaneous measurements of the frequency changes of an electrochemical quartz crystal microbalance (EQCM). First we investigated the adsorption of PEG_x on the surface of the Pt electrode at the open circuit potential. The results obtained showed that the mass of PEG_x adsorbed on the Pt surface reaches a stationary value with time, and that this stationary value increases in proportion to the PEG molecular weight. The quantity of PEG_x adsorbed on the Pt surface increased when Cl^- ions were present. In addition, the adsorption of PEG_x did not interfere with the oxidation of the Pt surface to form a PtO film. Analysis of simultaneously recorded voltammograms and massograms revealed that during the potential scan in the negative direction in solutions without Cl^- , three processes involving the partial desorption of PEG_x from the Pt surface. In the presence of Cl^- , by contrast, one adsorption process and two partial desorption processes of PEG_x occur. On the basis of the CV and EQCM data, we propose that in the absence of Cl^- ions, the oxidation of PEG_x in the potential interval from 0.5 to 0.8 V form the corresponding aldehyde adsorbed on the Pt surface. In the presence of Cl^- ions, however, the oxidation of PEG_x was almost completely suppressed.

Keywords: Adsorption, EQCM, massograms, polyethyleneglycol

1. INTRODUCTION

Polyethoxylated compounds are of great importance in the galvanoplastics industry, where they are principally used as additives in electrolytic baths. Additives have come to be indispensable components of electrolytic baths because their presence substantially improves the quality of the metal

coatings obtained. The advantageous effects of additives on the morphology and physical properties of metal coatings include the following: reduction of the grain size of the metallic crystals, which aids in the production of smooth, adherent and shiny coatings [1-4]; modification of the crystallographic orientation of the coating; and increased corrosion resistance [5]. The addition of certain polymers, for example polyethyleneglycol (PEG), to an electrolytic bath greatly improves the quality of the metal coatings obtained. The beneficial effects of polymer additives have motivated growing interest in the effects of these additives on the morphology and physical properties of the deposits. Generally the effects of polyethoxylated additives on the morphological characteristics of electrodeposited coatings principally stem from adsorption of the additive molecules on the electrode surface [6-9]. However, in spite of numerous studies of the effect of polyethoxylated compounds on coating characteristics, little is known about their adsorption mechanism on the electrode surface or their mode of action. Based on Raman spectroscopy data, Healy et al. [10,11] suggested that the type of PEG species adsorbed on the electrode surface depends on the applied potential. Specifically, they proposed that neutral PEG molecules are adsorbed at more negative potentials, where copper deposition occurs, while at potentials close to the open circuit potential, PEG adsorbs as a copper chloride complex with the polymer acting as a ligand analogous to a crown ether. In addition, measurements of the differential capacitance in H_2SO_4 electrolyte have shown that PEG is weakly adsorbed on the copper surface [12]. Similarly, Hope et al. [13] observed weak adsorption of PEG on steel during the electrodeposition of copper. The weakly adsorbed macromolecules are sufficiently mobile and remain trapped in the deposit by the approaching atomic layer, leading to the incorporation of aggregates rather than individual molecules. In studies using a quartz crystal microbalance and electrochemical impedance spectroscopy, Kelly and West [14,15] found that adding PEG alone to an electrolytic bath had only a small effect on the electrode kinetics, and that Cl^- alone promoted the copper deposition reaction. However, they found that when both PEG and Cl^- were present in the solution, the PEG monolayer collapses into spherical aggregates. Using ellipsometry, Bonou et al. [16] found that the adsorption of PEG on the electrode surface depended on the applied potential, with PEG not being adsorbed at the open circuit potential. In addition, various studies suggest that PEG adsorbed on the electrode surface forms a barrier [17] that inhibits metal deposition and increases the overpotential for the discharge of the metal ion, for example Zn [18,19] or Cu [20], and that the degree of inhibition increases with increasing the molecular weight of the polyethoxylated compound. Recently, Safonova et al. [21] found that in an H_2SO_4 electrolyte solution, PEG adsorption is accompanied by dehydrogenation and hydrogenation processes that likely involve the terminal groups of the polymer. In addition, Kim et al. [8] found that polyethoxylated compounds were adsorbed on an iron electrode surface in a more or less ordered arrangement, and were desorbed from the surface in the underpotential deposition region of zinc ions.

Given the importance of polyethoxylated compounds as additives in electrodeposition processes, we investigated the adsorption/desorption behavior of PEG molecules with various molecular weights as well as the coadsorption with Cl^- ions on the surface of a Pt electrode in a perchloric acid solution. This study was performed using cyclic voltammetry (CV) in conjunction with an electrochemical quartz crystal microbalance (EQCM).

2. EXPERIMENTAL

The study of PEG adsorption was performed using four solutions, comprised of base solution S_0 ($= 0.1 \text{ M HClO}_4$) with 10^{-6} M PEG_x ($x = 400, 3000, 8000, \text{ or } 20000$). The study of the coadsorption of PEG_x and Cl^- ions was performed using the above $S_0 + \text{PEG}_x$ solutions plus 10^{-3} M HCl . The solutions were prepared immediately before each electrochemical experiment from super-pure water ($18 \text{ M}\Omega \text{ cm}$) and analytical grade reagents purchased from J.T. Baker. Before each electrochemical experiment, the solutions were deoxygenated for 30 min with ultra-pure nitrogen (Praxair), and the experiments were carried out under a nitrogen atmosphere at $25 \pm 0.5^\circ\text{C}$.

The electrochemical and microgravimetric study was carried out in a conventional three-electrode cell with a water jacket. A quartz crystal microbalance (Maxtek Mod. 710) and a potentiostat/galvanostat (EG & G PAR Mod. 273A) controlled by independent computers running the software PM710 and EG & G M270, respectively, were used to simultaneously measure electrochemical parameters and the frequency of the quartz crystal. An AT-cut quartz crystal of nominal frequency $f_0 = 5 \text{ MHz}$, covered on both sides with Pt film (Maxtek, CA), was used as the working electrode (Pt-EQCM). The geometric area of the Pt-EQCM electrode was 1.37 cm^2 . The real area of the electrode was estimated to be 4.70 cm^2 from the desorption charge of UPD H and the charge corresponding to the desorption of a monolayer of H_{ads} from polycrystalline platinum (0.210 mC cm^{-2}) [22]. A saturated calomel electrode (SCE) and a graphite rod were used as the reference and counter electrodes, respectively. All potentials in this work are referred to SCE. In order to minimize iR-drop effects, a Luggin capillary was employed to connect the reference-electrode compartment to the working-electrode one.

The EQCM signal was recorded as Δf ($= f - f_{\text{initial}}$) as a function of the electrode potential. The experimental frequency change can be expressed as [23,24]:

$$\Delta f = -C_f \Delta m + \Delta f_\eta + \Delta f_r + \dots \quad (1)$$

where the first term on the right-hand side of Eq. (1) is the Sauerbrey term [25], which represents the total mass change at the electrode surface. Other possible contributions to the frequency change include changes in the solution viscosity [26] and the surface roughness [27]. In the present work, the use of polished Pt-EQCM electrodes (roughness 1.171 nm , as measured by AFM) should minimize the effects of surface roughness, and the effects of viscosity variations are expected to be negligible. Prior to the measurements, the sensitivity factor ($C_f = 0.042 \text{ Hz ng}^{-1} \text{ cm}^2$) of the quartz crystal was determined using the chronoamperometry calibration method described by Vatankhah et al. [28].

3. RESULTS AND DISCUSSION

3.1. Characterization of the surface of the Pt-EQCM electrode

Prior to each experiment, the Pt-EQCM electrode was cycled between -0.25 and 1.2 V in 0.1 M HClO_4 solution until a reproducible voltammetric profile was obtained. The quality of the electrode

and the purity of the electrolyte solution were verified by recording CV profiles and comparing them with previously reported profiles for this system [22]. Fig. 1 (curve a) shows a typical cyclic voltammogram of Pt in this medium, which is consistent with previously reported voltammograms for this system [29].

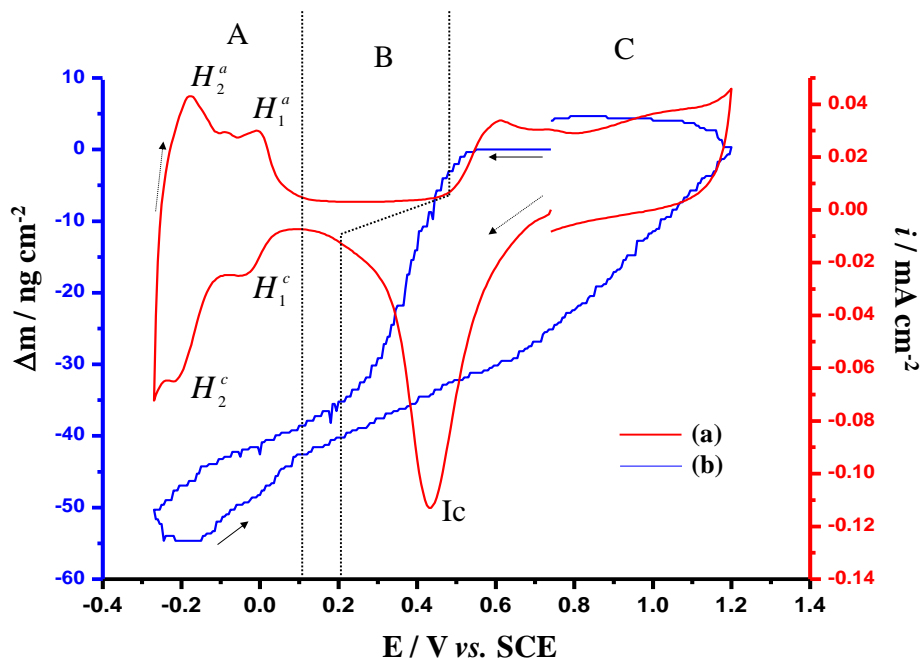
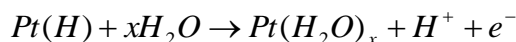


Figure 1. (a) Cyclic voltammogram and (b) Δm vs E plot for a Pt-EQCM electrode in solution S_0 ($= 0.1 \text{ M HClO}_4$), $v = 50 \text{ mV s}^{-1}$.

Three characteristic regions are observed, denoted A, B and C. In region A (-0.25 to 0.1 V), the process of UPD H is characterized by the cathodic peaks H_1^c and H_2^c associated with two types of adsorbed hydrogen (H_{ads}): strongly and weakly bound H respectively [30]. Peaks H_1^a and H_2^a are the anodic equivalents of H_1^c and H_2^c . Region B (0.1 to 0.5 V) corresponds to the double layer region, while region C (0.5 to 1.2 V) is associated with the formation and reduction (Peak Ic) of a film of platinum oxide (PtO) on the surface. Curve b shows the change in mass per unit area (Δm) on the electrode surface simultaneously measured by EQCM during the recording of the voltammogram. The variation in Δm of Pt-EQCM electrodes in HClO_4 solutions as a function of potential has been studied by various groups [31-33]. During the potential scan in the negative direction in regions C and B, Δm decreases (mass loss) due to the reduction of the oxide film (PtO) and anion desorption, respectively [29]. In region A, the mass loss is associated with the adsorption of hydrogen (H_{ads}) and the desorption of water molecules. During the potential scan in the positive direction, on the other hand, Δm increases (mass gain) in region A, even though the UPD H is desorbed from the electrode surface in this potential range. This increase in Δm derives from the adsorption of water molecules in the active sites formerly occupied by hydrogen atoms (H_{ads}). The increase in mass during the desorption of UPD H has been discussed by Gloguen et al. [34], who observed very similar mass shift behavior for both

perchlorate and bisulfate ions. They suggested that this mass increase is produced by the substitution of H with water molecules according to the following reaction scheme:



and is not due to adsorption of perchlorate or bisulfate. In the double layer region, on the other hand, increases in Δm have frequently been associated with the adsorption of ClO_4^- ions [30] and of water molecules [28]. In region C, the mass increase observed in the potential scan in the positive direction is due to Pt surface oxidation [35].

3.2. Study of the adsorption of PEG with different molecular weights on Pt-EQCM

3.2.1. Adsorption of polyethyleneglycol on the Pt-EQCM electrode at the open circuit potential (E_{OCP})

The study was carried out using four base solutions comprised of S_0 ($= 0.1 \text{ M HClO}_4$) with 10^{-6} M PEG_x ($x = 400, 3000, 8000$ or 20000 g mol^{-1}). After the frequency of the microbalance had remained stable for 2 min, the PEG_x was injected in the electrolytic solution S_0 with constant agitation. The change in the resonant frequency of the quartz crystal was recorded for 4 min following the addition of the polymer to monitor the adsorption of the additive.

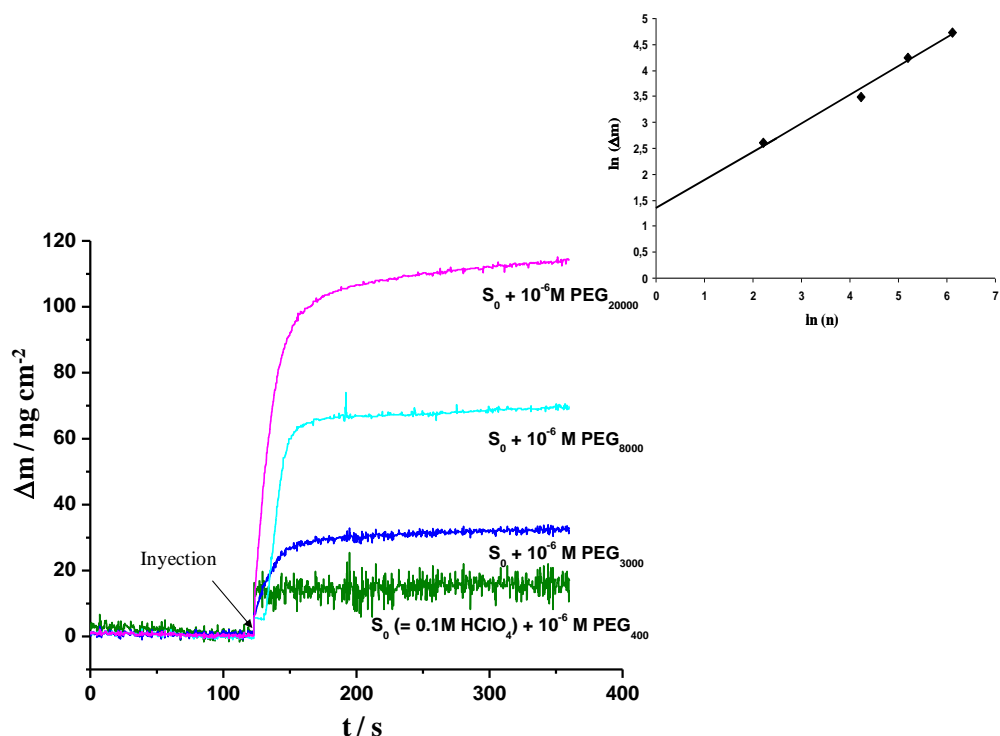


Figure 2. Mass change (Δm) as a function of time after adding PEG_x to solution S_0 . The final concentration in the solution was: S_0 ($= 0.1 \text{ M HClO}_4$) + 10^{-6} M PEG_x ($x = 400, 3000, 8000$, or 20000 g mol^{-1}). The experiments were carried out at the open circuit potential ($E_{OCP} = 0.65 \text{ V}$ vs. SCE). Inset: $\ln(\Delta m)$ vs. $\ln(n)$, where n is the number of monomer units.

Fig. 2 shows the mass changes (calculated using Eq. 1) recorded for each solution. Immediately after adding the PEG_X, the mass on the electrode surface increases rapidly; the magnitude of the mass change increasing as the molecular weight of the injected PEG_X increases. In addition, the mass changes for the three polymers of lower molecular weight, PEG_X ($x = 400, 3000$, and 8000), rapidly reach a stationary state; whereas PEG₂₀₀₀₀ requires a longer time to stabilize. In a previous study using EQCM and STM, Kim et al. [8] showed that after the initial rapid rise in mass of polymer adsorbed on the quartz crystal surface, the adsorbed polymer layer enters a stabilization phase in which the adsorbed PEG molecules are rearranged into more ordered structures.

In addition, in agreement with Kelly and West [14], the change in mass on the electrode surface is proportional to the number of repeat units in the polymer, which in turn is proportional to the molecular weight, that is:

$$\Delta f \propto \Delta m \propto n^{\beta} \quad (2)$$

where n is the number of repeat units in the polymer. The inset of Fig. 2 shows a plot of $\ln \Delta m$ vs. $\ln n$; a least squares fit of the data shows linear behavior with a slope of $\beta (= 0.58)$. Previous studies [14,36] have reported that when $0.5 \leq \beta \leq 1$, the PEG_X molecules collapse in a parking arrangement such as so-called polymer brushes, where a portion of each polymer molecule dangles into the solution.

3.2.2. Cyclic voltammetry study

Immediately after the 4-min period in which the PEG_X adsorbed onto the Pt-EQCM electrode at E_{OCP} , we simultaneously performed CV and EQCM studies for each of the PEG_X polymers considered. The potential scan was started in the negative direction from E_{OCP} , over the potential range -0.25 to 1.2 V.

Fig. 3 shows a series of typical voltammograms obtained under these conditions. Curve a shows the voltammogram for Pt in solution S₀. (These data were presented above in Fig. 1, and are included in Fig. 3 for comparison purposes). The electric charge density for the desorption of hydrogen, obtained by integration of the anodic current density in region A of curve a, was 0.157 mC cm^{-2} , after correcting for the double layer charge. Similarly, an electric charge density of 0.474 mC cm^{-2} was obtained by integrating the anodic current in regions B and C (0.1 to 1.2 V); this charge density is associated with the double layer charge and oxidation of the electrode surface to form PtO.

The addition of PEG_X to the base solution S₀ caused significant changes in the voltammogram profiles (curves b-e). In [21] as well as the present study, the intensity of peak Ic, associated with the reduction of the PtO film on the surface, is approximately the same for all solutions both with and without the polyethoxylated compounds, indicating that the adsorption of PEG_X on the electrode surface does not interfere with the formation of the oxide film. In region A (-0.25 to 0.1 V) the presence of PEG_X causes a decrease in the current density (cathodic and anodic) associated with the adsorption and desorption of hydrogen, principally that arising from strongly bonded hydrogen (H_1^c)

and H_1^a). This behavior is similar to that observed by Safonova et al. [21] in a study of the adsorption of PEG on Pt/Pt in H_2SO_4 solutions. However, contrary to the findings of Safonova, we found that this effect became more pronounced with increasing molecular weight of the PEG_x in solution S_0 . Under the conditions studied, the current density associated with the adsorption-desorption processes of UPD H was not completely suppressed, indicating that the additive adsorbed on the surface of the Pt-EQCM electrode blocked only a fraction of active sites for the adsorption of hydrogen. In addition, the potential range corresponding to region B in the anodic part of the voltammogram decreases as the molecular weight of the PEG_x is increased due to the formation of the anodic peak P1 at around 0.5 V. The intensity of peak P1 increases with the molecular weight of PEG_x , indicating that this peak is associated with the oxidation of PEG_x .

Additional experiments varying the concentration of PEG_x showed that the current density of peak P1 (i_{p1}) increases more or less linearly with the PEG concentration. These results showed that the oxidation process is controlled by diffusion of the electroactive species and that an additional process exists that may be associated with the quantity of PEG_x that remains adsorbed on the electrode surface after the potential scan in the negative direction.

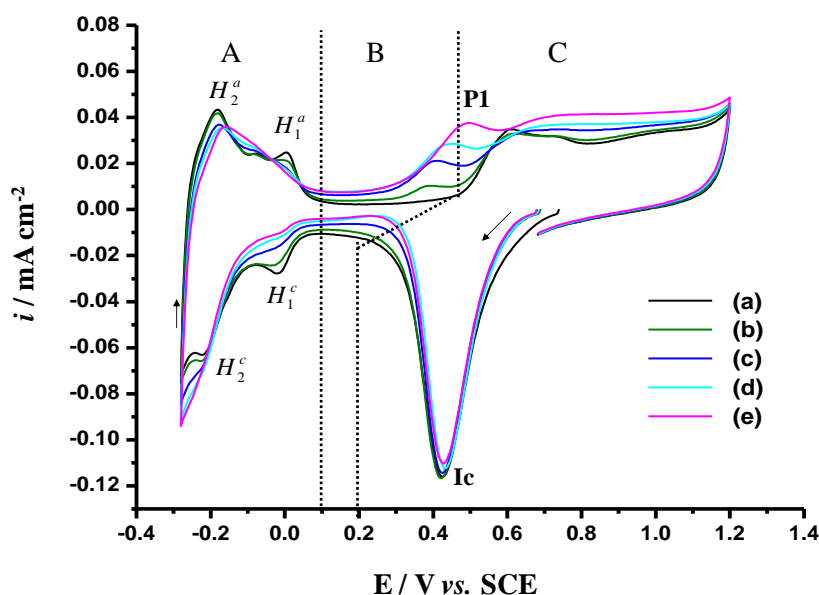


Figure 3. Cyclic voltammograms of a Pt-EQCM electrode in solutions $S_0 + 10^{-6} \text{ M } \text{PEG}_x$. (a) S_0 , (b) $x = 400$, (c) $x = 3000$, (d) $x = 8000$, (e) $x = 20000 \text{ g mol}^{-1}$. $v = 50 \text{ mV s}^{-1}$.

The inhibition of the desorption of hydrogen (region A) by adsorbed PEG_x , after the potential scan in the negative direction, can be used as a measure to estimate the degree of coating of the surface by adsorbed PEG_x molecules ($\Theta_{ads}^{PEG_x}$) using the following equation:

$$\Theta_{ads}^{PEG_x} = \frac{Q_H - Q_H^{PEG_x}}{Q_H} \quad (3)$$

where Q_H and $Q_H^{PEG_x}$ are the electric charge densities (mC cm^{-2}) associated with the desorption of hydrogen (region A) in the absence and presence of PEG_X respectively. Thus, the difference between Q_H and $Q_H^{PEG_x}$ is proportional to the number of active sites for the desorption of hydrogen that are blocked by PEG_X molecules that remain adsorbed after the potential scan in the negative direction starting from E_{OCP} . The charge densities can be obtained by integrating the voltammetric current density (Fig. 3) in the corresponding potential interval, using the following general equation:

$$Q = \int_{E_i}^{E_s} \frac{|i|}{v} dE \quad (4)$$

where $v (= 0.05 \text{ V s}^{-1})$ is the potential scan rate.

Table 1 shows the values of $\Theta_{ads}^{PEG_x}$ for the various molecular weights of PEG_X . The value of $\Theta_{ads}^{PEG_x}$ increases with increasing molecular weight of PEG_X , reaching a maximum of 0.217 for PEG_{20000} . The calculated values of $\Theta_{ads}^{PEG_x}$ are less than the values of up to 0.6 reported by Safonova et al. [21]. This difference may be due to the greater porosity of a Pt/Pt electrode in comparison to a smooth platinum electrode.

The difference in the anodic charge density, measured from the voltammograms obtained in the presence ($Q_{(0.1 \text{ to } 0.6V)}^{Ox}$) and absence of PEG_X (0.085 mC cm^{-2}) in the potential range 0.1 to 0.6 V, is associated with the oxidation of PEG_X molecules ($Q_{(0.1 \text{ to } 0.6V)}^{Ox, PEG_x} = Q_{(0.1 \text{ to } 0.6V)}^{Ox} - 0.085 \text{ mC cm}^{-2}$). Table 1 shows the estimated values of the charge density associated with the oxidation of PEG_X ($Q_{(0.1 \text{ to } 0.6V)}^{Ox, PEG_x}$) for various molecular weights of the polyethoxylated compound in the base solution (S_0). For the same moles number of PEG_X , the $Q_{(0.1 \text{ to } 0.6V)}^{Ox, PEG_x}$ value increase with increasing the molecular weight of the polyethoxylated compound. This behavior is equivalent to the expected when the concentration increases, and is indicative of the possible scission of the PEG_X molecules in acid medium [17].

Table 1. Variation in the charge density (Q) during the potential scan in the positive direction in different regions of the voltammograms in Fig. 3. The values of the degree of coating of the Pt surface ($\Theta_{ads}^{PEG_x}$) are also listed.

$\text{HClO}_4 (0.1\text{M}) + 10^{-6} \text{ M PEG}_X$	$Q_H^{PEG_x}$ (mC cm^{-2})	$\Theta_{ads}^{PEG_x}$	$Q_{(0.1 \text{ to } 0.6V)}^{Ox}$ (mC cm^{-2})	$Q_{(0.1 \text{ to } 0.6V)}^{Ox, PEG_x}$ (mC cm^{-2})
X = 400	0.148	0.057	0.110	0.025
3000	0.133	0.152	0.156	0.071
8000	0.130	0.172	0.188	0.103
20000	0.123	0.217	0.210	0.125

Without PEG: $Q_H = 0.157 \text{ mC cm}^{-2}$, $Q_{(0.1 \text{ to } 0.6V)} = 0.085 \text{ mC cm}^{-2}$

3.2.3. EQCM Study

The EQCM experiments were carried out simultaneously with the voltammetry measurements, immediately after the adsorption of the polyethoxylated compound on the Pt-EQCM surface at E_{OCP} . The EQCM data are presented as plots of $d\Delta m / dt^l$ vs. E , known as massograms [37-40], where $d\Delta m / dt^l$ is the rate of change of the mass (mass flux) at the electrode surface. For changes in mass associated with charge transfer at the electrode surface (faradaic processes), $d\Delta m / dt^l$ is directly proportional to the current density and hence the massogram is analogous to the voltammogram. In addition, given that observation of a mass flux in the massogram without a corresponding current density in the voltammogram is evidence of a nonfaradaic mass change (i.e., a mass change without an associated charge transfer) on the electrode surface, it is possible to distinguish between faradaic and nonfaradaic processes by comparing a massogram with its corresponding voltammogram.

In the massograms, negative mass flux ($-d\Delta m / dt^l$) corresponds to the loss of mass at the electrode surface, while positive mass flux ($d\Delta m / dt^l$) corresponds to mass gain at the electrode surface. Fig. 4 shows the family of massograms corresponding to the voltammograms in Fig. 3. At the beginning of the potential scan in the negative direction starting from E_{OCP} , a peak of negative mass flux (peak I'c), associated with the loss of mass due to the reduction of the PtO film, is observed. It is important to emphasize that the intensity of this peak increases with increasing PEG_x molecular weight, which differs from the behavior observed for cathodic peak Ic in the corresponding voltammograms (Fig. 3), which exhibited similar current densities for all solutions, regardless of the PEG_x molecular weight. This finding suggests that the increase in mass loss in this potential region is due to a nonfaradaic process corresponding to the desorption of PEG_x adsorbed on the PtO film. When the PtO film is reduced, PEG_x is desorbed from the film. At potentials less positive than the potential of peak I'c, another peak, I'c₁ (0.25 V), is observed whose intensity increases with increasing PEG_x molecular weight. It is important to note that no cathodic current density associated with this process exists in the voltammograms (Fig. 3), which suggests that the mass loss corresponding to peak I'c₁ is due to a nonfaradaic process. In the potential region -0.25 to -0.1 V a new process with negative mass flux is observed, which corresponds to the replacement of water molecules with H_{ads} . It is important to point out that in the voltammogram in Fig. 3, an increase in the cathodic current density is observed in the same potential range, suggesting that the loss of mass detected by EQCM may contain a contribution from the product of the reduction of adsorbed PEG_x molecules.

The quantity of mass lost due to the desorption of PEG_x from the electrode surface during the potential scan in the negative direction can be calculated from the difference between the mass changes obtained by integrating the mass fluxes in the massograms in the presence and absence of PEG_x , using the following equation:

$$\Delta m_{(0.65 \text{ to } -0.25V)}^{Cathodic} = \int_{E_{OCP}=0.65V}^{E_2=-0.25V} \left(\frac{d\Delta m}{dt} \right)^{\text{With } PEG_x} \frac{1}{v} dE - \int_{E_{OCP}=0.65V}^{E_2=-0.25V} \left(\frac{d\Delta m}{dt} \right)^{\text{Without } PEG_x} \frac{1}{v} dE \quad (5)$$

with $v = 0.05 \text{ V s}^{-1}$

where the first term on the right hand side of the equation represents the mass loss (desorption) in the presence of PEG_x and the second term corresponds to the mass loss in the absence of PEG_x , during the potential scan in the negative direction in the indicated potential interval.

Table 2 lists the values of $\Delta m_{(0.65 \text{ to } -0.25V)}^{\text{Cathodic}}$ for the various systems. The mass desorbed from the electrode surface increases with the PEG molecular weight. In addition, the difference between the mass adsorbed at the open circuit potential (Δm_{OCP}) and the absolute value of the mass desorbed during the potential scan in the negative direction ($|\Delta m_{(0.65 \text{ to } -0.25V)}^{\text{Cathodic}}|$) suggests that some PEG_x ($\Delta m_{\text{Ads}}^{\text{PEG}_x}$) remains adsorbed on the Pt-EQCM surface after the potential scan in the negative direction, and that the mass of this remaining PEG_x increases with the molecular weight. This remaining adsorbed PEG_x blocks partially the active sites and therefore a fraction of the electrode surface.

$$\Delta m_{\text{ads}}^{\text{PEG}_x} = \Delta m_{OCP} - |\Delta m_{(0.65 \text{ to } -0.25V)}^{\text{Cathodic}}| \quad (6)$$

In region B of the anodic part of the massograms, the beginning of the formation of the peak P'1 of positive mass flux is observed (i.e., a mass gain). The potential of this peak ($E_{P'1}$) is 0.5 V, which is similar to the peak potential of the oxidation process observed in the voltammogram (Peak P1, Fig. 3); thus, the mass increase observed in the massogram can be assigned to the adsorption of the product of the oxidation of PEG_x that occurred during the potential scan in the positive direction. The mass gain observed in the potential interval 0.1 to 0.6 V was quantified from the massograms in Fig. 4, using the following equation:

$$\Delta m_{(0.1 \text{ to } 0.6V)}^{\text{Anodic}} = \int_{E_i=0.1V}^{E_2=0.6V} \left(\frac{d\Delta m}{dt} \right)^{\text{with } \text{PEG}_x} \frac{1}{v} dE - \int_{E_i=0.1V}^{E_2=0.6V} \left(\frac{d\Delta m}{dt} \right)^{\text{without } \text{PEG}_x} \frac{1}{v} dE \quad (7)$$

with $v = 0.05 \text{ V s}^{-1}$

Table 2 lists the values of the mass gain, $\Delta m_{(0.1 \text{ to } 0.6V)}^{\text{Anodic}}$, obtained during the potential scan in the positive direction in the interval 0.1 to 0.6 V as a function of the PEG molecular weight. It is observed that $\Delta m_{(0.1 \text{ to } 0.6V)}^{\text{Anodic}}$ increases with the molecular weight of PEG_x .

From the mass gain ($\Delta m_{(0.1 \text{ to } 0.6V)}^{\text{Anodic}}$) (Table 2) in the potential interval 0.1 to 0.6 V and the charge consumed during the potential scan in the positive direction ($Q_{(0.1 \text{ to } 0.6V)}^{\text{Ox,PEG}_x}$) (Table 1) in the same potential interval, it is possible to calculate the apparent molar mass of the species formed during the oxidation of PEG_x , using the following equation (Eq. 8).

$$\frac{PM}{n} = \frac{\Delta m_{(0.1 \text{ to } 0.6V)}^{\text{Anodic}}}{Q_{(0.1 \text{ to } 0.6V)}^{\text{Ox,PEG}_x}} F \quad (8)$$

where PM is the molecular weight of the species formed, n is the number of electrons transferred, and F is Faraday's constant.

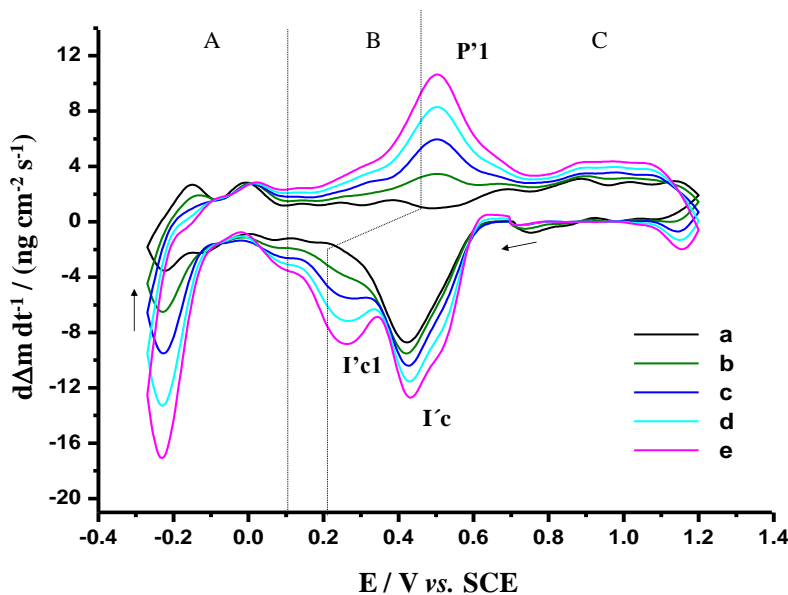


Figure 4. A series of massograms obtained at the same time as the cyclic voltammograms in Fig. 3, for solutions of composition $S_0 + 10^{-6}$ M PEG_x . (a) S_0 , (b) $x = 400$, (c) $x = 3000$, (d) $x = 8000$, (e) $x = 20000 \text{ g mol}^{-1}$. $v = 50 \text{ mV s}^{-1}$.

Table 2 lists the results obtained for each of the PEG_x molecular weights used. With the exception of PEG_{400} , the value of the ratio PM/n is similar for the different PEG_x molecular weights, with a mean value of $44.66 \pm 3.12 \text{ g mol}^{-1}$. This finding suggests the simultaneous oxidation and adsorption of PEG_x , leading to the formation of the corresponding aldehyde by transfer of 2 electrons. Considering the model of PEG_{1000} adsorption on Fe(110) proposed by Kim et al. [8], in which the PEG_{1000} molecules are adsorbed in a planar configuration via the oxygen atoms, the PM calculated in the present work ($\sim 90 \text{ g mol}^{-1}$) corresponds to the molecular weight of the number of oxygen atoms (approximately 6) that are adsorbed into Pt-QCM electrode surface, in accordance with the following reaction:



Is quite possible that the species $[\text{HO} - (\text{CH}_2 - \text{CH}_2 - \text{O} -)_n \text{CH}_2 - \text{CH}_2\text{OH}]$ is present in the solution. For PEG as an additive, the question of the most relevant chain length is still open, as the PEG_x ($X > 400$) molecules are degraded in the acidic electrolyte [17]. The products of this scission process are PEG units with an average of length chain of around 20, some of which are adsorbed on the electrode surface, likely via their oxygen atoms, in a packed arrangement such as the so-called polymer brushes. During the potential scan in the negative direction, some of these molecules are

desorbed from the electrode surface, while the remaining molecules remain adsorbed. During the potential scan in the positive direction, a majority of the PEG molecules, including both those adsorbed on the electrode surface and those in solution, are oxidized to form the corresponding aldehyde molecules, which remain adsorbed on the electrode surface. Thus, the mass gain observed at the potential 0.5 V corresponds principally to the adsorption of the corresponding aldehyde formed by oxidation of PEG units.

Table 2. Mass changes (Δm) in different potential ranges in the massograms in Fig. 4. The values of the ratio PM/n for different PEG_x molecular weights are also listed.

$HClO_4$ (0.1M) + 10^{-6} M PEG_x	$\left \Delta m_{(0.65 \text{ to } -0.25V)}^{\text{Cathodic}} \right $	Δm_{OCP}	$\Delta m_{ads}^{PEG_x}$	$\Delta m_{(0.1 \text{ to } 0.6V)}^{\text{Anodic}}$	PM/n
	(ng cm ⁻²)	(ng cm ⁻²)	(ng cm ⁻²)	(ng cm ⁻²)	(g mol ⁻¹)
X = 400	16.0	16.17	0.17	16.10	62.13
3000	32.6	38.97	6.37	31.31	42.54
8000	50.4	69.23	18.83	46.57	43.74
20000	68.3	113.46	45.16	61.83	47.72

3.3. Coadsorption of PEG_x and Cl^- ions on the Pt-EQCM

This study was carried out using solutions formed by simultaneously adding the necessary quantities of HCl (conc.) and PEG_x (10^{-2} M) to the base solution S_0 so as to obtain a final composition of S_0 ($= 0.1$ M $HClO_4$) + 10^{-3} M HCl + 10^{-6} M PEG_x . The HCl and PEG_x were added to S_0 with constant agitation over a period of 4 min to permit the adsorption of Cl^- ions and PEG_x on the electrode surface. Immediately after this period, the CV and EQCM study was performed. Cyclic voltammograms were recorded over the potential range -0.25 to 1.2 V, starting in a negative direction from E_{OCP} . The voltammetric data were compared with the simultaneously recorded massograms. The effect of the Cl^- ions on the adsorption of PEG_x at the open circuit potential, E_{OCP} , is evident in Fig. 5, which shows the changes in mass recorded during the adsorption of PEG_{8000} in the absence and presence of Cl^- ions. In the presence of Cl^- ions, the quantity of PEG_{8000} adsorbed increases considerably (128%). This result is in agreement with the findings of Kelly and West [14], who proposed that Cl^- ions promote the adsorption of PEG.

3.3.1. Cyclic voltammetry study

Fig. 6 shows a series of voltammograms for solutions with compositions of S_0 , $S_0 + 10^{-3}$ M HCl , and $S_0 + 10^{-3}$ M $HCl + 10^{-6}$ M PEG_x ($x = 400, 3000, 8000$, or 20000). The voltammogram

obtained for the $S_0 + 10^{-3}$ M HCl solution (curve b) shows behavior characteristic of Pt-EQCM in such media [31]. In the region UPD H, the Cl^- ions induce a redistribution of the electrodeposited H between the different states of H adsorption in clean acid solutions; principally the displacement of peaks H_1^c and H_1^a toward negative potentials is observed, forming the peaks H_1^c and H_1^a . In addition, the Cl^- ions block the first stage (to 0.80 V) of formation of oxide film (Pt/O)[33].

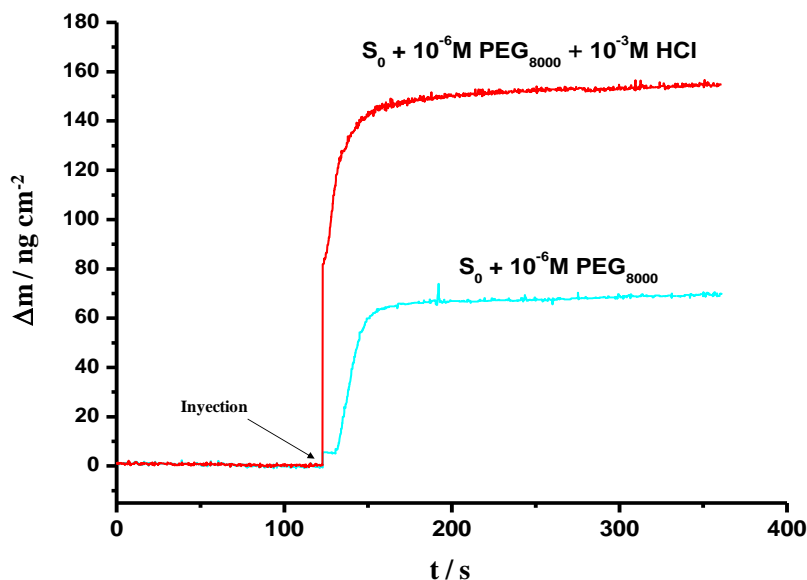


Figure 5. Mass change (Δm) as a function of time after adding HCl and PEG_{8000} to solution S_0 . The final concentration in the solution was: S_0 ($= 0.1 \text{ M HClO}_4 + 10^{-3} \text{ M HCl} + 10^{-6} \text{ M PEG}_{8000}$). The experiments were carried out at the open circuit potential ($E_{\text{OCP}} = 0.65 \text{ V vs. SCE}$). Also shown is the change in mass on the electrode surface after adding $10^{-6} \text{ M PEG}_{8000}$ alone to solution S_0 .

It is important to note that at the beginning of the potential scan in the negative direction, the intensity of the peak associated with the reduction of the PtO film (peak Ic) is similar for the solutions without and with Cl^- ions (curves a and b respectively), which indicates that under these conditions the Cl^- ions do not interfere with the formation of the oxide film on the surface.

When both Cl^- ions and PEG_x are added to solution S_0 , however, significant changes are observed in the voltammograms (curves c-f) compared to the voltammogram obtained in the presence of Cl^- alone. Specifically, in the cathodic part of region A, the gradual suppression of the peak associated with the adsorption of hydrogen H_1^c is observed with increasing the molecular weight of PEG_x . In addition, a slight decrease is observed in the intensity of the peak associated with the reduction of the PtO film (peak Ic). Moreover, in the anodic part of region A, a decrease is observed in the intensity of the peaks associated with the desorption of H (H_1^a and H_2^a), in particular in peak H_1^a . In region B corresponding to the region of the double layer charge, an increase in the current density occurs due to the adsorption of Cl^- ions and PEG_x molecules. In addition, in the potential interval 0.5

to 0.80 V (which corresponds to the formation of the initial states of the oxide film), the current density is greater than was observed in the presence of Cl^- ions alone (curve b) and increases with increasing molecular weight of PEG_x ; this increase may be associated with the oxidation of PEG_x molecules or the formation of the oxide film in its initial state. At potentials above 0.8 V similar behavior is observed.

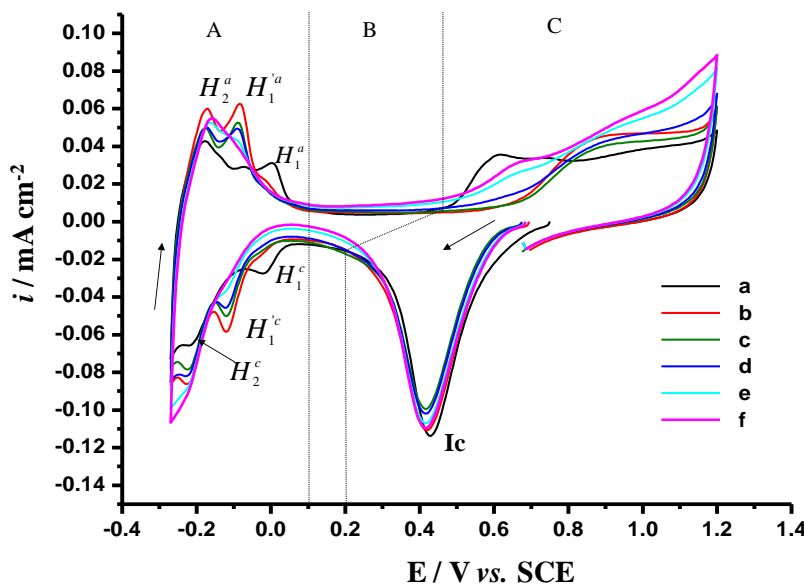


Figure 6. Cyclic voltammograms of a Pt-EQCM electrode in solutions: (a) S_0 , (b) $S_0 + 10^{-3}$ M HCl , and $S_0 + 10^{-3}$ M $\text{HCl} + 10^{-6}$ M PEG_x . (c) $x = 400$, (d) $x = 3000$, (e) $x = 8000$, (f) $x = 20000$ g mol^{-1} . $v = 50$ mV s^{-1} .

In order to determine the nature of the increase in anodic current density in the potential interval 0.5 to 0.80 V, we performed CV experiments with two potential scan cycles. Fig. 7 shows the voltammograms obtained for solutions S_0 (curve a), $S_1 (= S_0 + 10^{-3}$ M $\text{Cl}^-)$ (curve b) and $S_2 (= S_0 + 10^{-3}$ M $\text{Cl}^- + 10^{-6}$ M PEG_{20000}) (curve c). The behavior of the voltammograms in the first potential scan cycle was already described above. At the commencement of the second cycle in the negative direction, peak Ic is observed for both solutions S_1 and S_2 (curves b and c respectively); however, this peak is considerably less intense than the peak observed in the first cycle, with solutions S_1 and S_2 showing similar reductions in intensity. The observation of a similar reduction in the magnitude of peak Ic between the first and second cycles for solutions S_1 and S_2 , suggests that this intensity decrease is associated with the inhibition of the formation of the oxide film in its initial state, due to the adsorption of Cl^- ions on the electrode in region B during the potential scan in the positive direction in the first cycle. Thus, this result leads us to conclude that the anodic current density observed in the presence of Cl^- ions and PEG_x (curves c-f, Fig. 6) in the interval 0.5 to 0.80 V does not correspond to the formation of the surface oxide, but rather to the oxidation of a quantity of PEG_x adsorbed on the surface of the Pt-EQCM electrode.

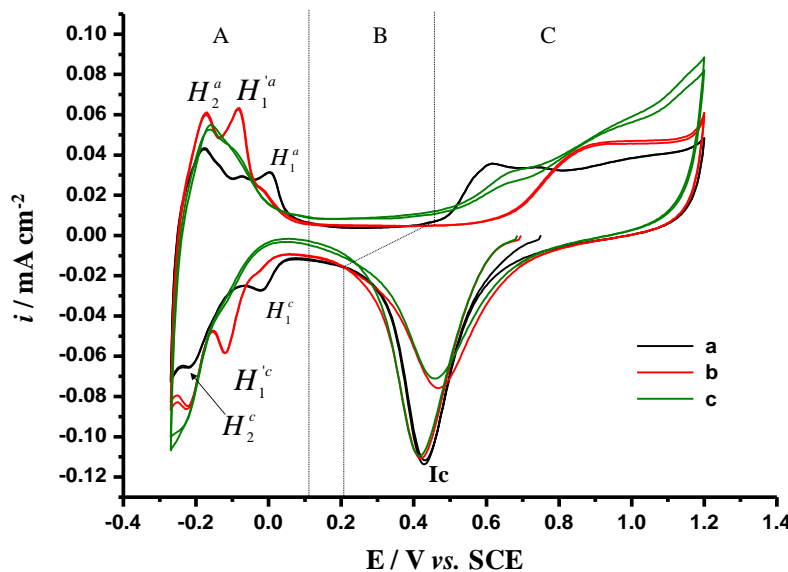


Figure 7. Cyclic voltammograms of a Pt-EQCM electrode in solutions: (a) S_0 , (b) $S_0 + 10^{-3}$ M HCl, (c) $S_0 + 10^{-3}$ M HCl + 10^{-6} M PEG₂₀₀₀₀. Two potential scan cycles are shown. $v = 50$ mV s⁻¹.

Table 3 lists the results obtained for the fraction of the electrode surface covered in the presence of Cl⁻ ions and PEG_X ($\Theta_{ads}^{PEG_x-Cl^-} = (Q_H^{Cl^-} - Q_H^{PEG_x-Cl^-})/Q_H^{Cl^-}$). The values of $\Theta_{ads}^{PEG_x-Cl^-}$ are greater than those obtained in the absence of Cl⁻ ions (Table 1). In addition, the charge associated at the PEG_X oxidation in the interval 0.1 to 0.80 V ($Q_{(0.1 \text{ to } 0.80 \text{ V})}^{Ox, PEG_x-Cl^-} = Q_{0.1 \text{ to } 0.80 \text{ V}}^{anodic PEG_x-Cl^-} - Q_{0.1 \text{ to } 0.80 \text{ V}}^{anodic Cl^-}$), increases with the molecular weight of PEG_X. The comparison between the values of charge density of the PEG_X oxidation; in the absence (table 1) and presence (table 3) of Cl⁻ ions, shows that the presence of Cl⁻ ions suppressed almost completely the PEG_X oxidation.

Table 3. Values of the anodic charge density in different potential ranges, obtained from the voltammograms in Fig. 6. The values of the mass change ($\Delta m_{(0.65 \text{ to } -0.25 \text{ V})}^{cathodic, PEG_x-Cl^-}$) obtained from Fig. 7 are also listed.

$HClO_4 (0.1M) + 10^{-6} \text{ M PEG}_x + 10^{-3} \text{ M Cl}^-$	$Q_H^{PEG_x-Cl^-}$ (mC cm ⁻²)	$\Theta_{ads}^{PEG_x-Cl^-}$ (mC cm ⁻²)	$\Delta m_{(0.65 \text{ to } -0.24 \text{ V})}^{cathodic PEG_x-Cl^-}$ (ng cm ⁻²)	$Q_{(0.1 \text{ to } 0.80 \text{ V})}^{anodic PEG_x-Cl^-}$ (mC cm ⁻²)	$Q_{(0.1 \text{ to } 0.80 \text{ V})}^{Ox. PEG-Cl^-}$ (mC cm ⁻²)
X = 400	0.147	0.22	0.173	0.095	- 0.009
3000	0.142	0.25	23.61	0.108	0.004
8000	0.133	0.30	71.17	0.150	0.046
20000	0.129	0.32	94.97	0.171	0.067

$$Q_H^{Cl^-} = 0.189 \text{ mC cm}^{-2} \quad Q_{0.1 \text{ to } 0.80 \text{ V}}^{anodic, Cl^-} = 0.104 \text{ mC cm}^{-2}$$

3.3.2. EQCM study

Fig. 8 shows the massograms corresponding to the voltammograms in Fig. 6. Comparison of these massograms with those obtained in the absence of Cl^- ions (Fig. 4) reveals the following differences: In the presence of Cl^- ions, the intensity of peak I'c in the part of the massogram with negative mass flux is greater than was observed in the corresponding massograms obtained in the absence of Cl^- (Fig. 4). That is, the quantity of PEG_x desorbed to give peak I'c is greater when Cl^- ions are present, which can be attributed to the fact that the presence of Cl^- ions enhances the quantity of PEG_x adsorbed. In addition, peak I'c₁ (mass loss) observed in the absence of Cl^- in the potential interval 0.15 to 0.35 V (Fig. 4) is suppressed in the presence of Cl^- ; in its place, a positive mass flux (mass gain) is observed for PEG_x with molecular weights greater than 3000. These findings indicate that in the presence of Cl^- and PEG_x with molecular weight > 3000, one adsorption process and two partial desorption processes occur at the surface of the Pt-EQCM electrode during the potential scan in the negative direction. The quantities of mass desorbed during the potential scan in the negative direction ($\Delta m_{(0.65 \text{ to } -0.24\text{V})}^{\text{cathodic,PEG}_x-\text{Cl}^-}$) from E_{OCP} for the various solutions are listed in Table 3. Comparing the quantity of mass desorbed for the systems with and without Cl^- in the solution, we find that in the presence of Cl^- , a greater mass is desorbed for solutions containing PEG molecular weights in excess of 3000. Thus, the Cl^- ions in solution promote the adsorption and desorption of PEG_x from the electrode surface.

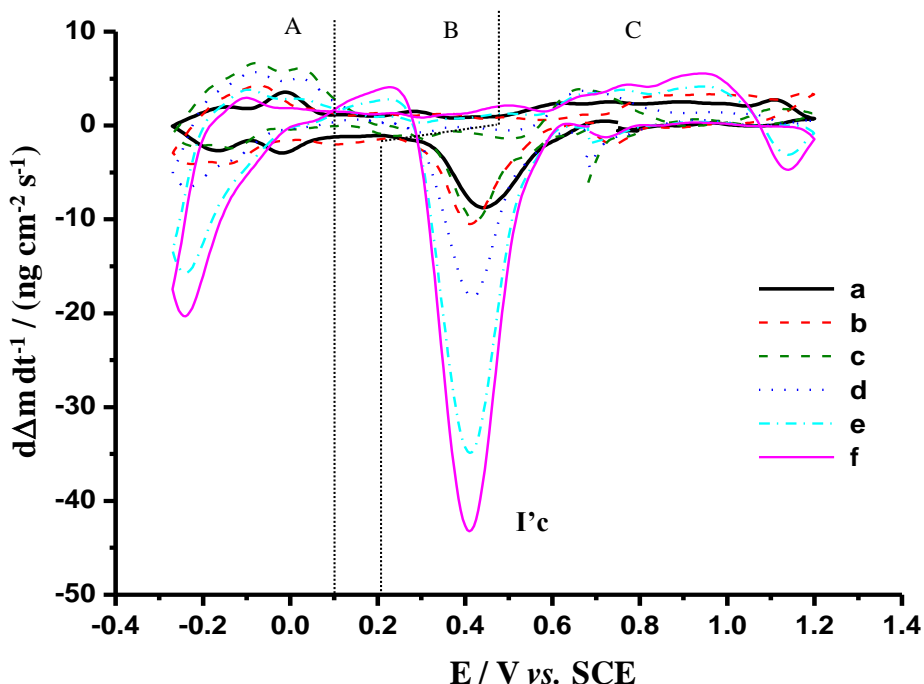


Figure 8. A series of massograms obtained at the same time as the cyclic voltammograms in Fig. 6, for solutions: (a) S_0 , (b) $S_0 + 10^{-3}$ M HCl, and $S_0 + 10^{-3}$ M HCl + 10^{-6} M PEG_x . (c) $x = 400$, (d) $x = 3000$, (e) $x = 8000$, (f) $x = 20000$ g mol⁻¹. $v = 50$ mV s⁻¹.

In the part of the massogram with positive mass flux, the peak P'1 observed in the absence of Cl^- ions (Fig. 4) in the potential interval 0.5 to 0.80 V which corresponds to the mass gain due to the oxidation of PEG_X molecules both in solution and adsorbed on the electrode, is suppressed when Cl^- are present in the solution, a finding similar to the results reported by Bahena et al. [38]. Based on this result, combined with the increase in anodic current density observed in the voltammograms in Fig. 6 in the same potential interval, we propose that in this potential interval the Cl^- ions suppress the oxidation of PEG_X molecules in solution but not those adsorbed on the electrode surface. This hypothesis is supported by the observation that the observed current density corresponds to the oxidation of PEG units that remained adsorbed on the Pt-EQCM surface after the first potential scan in the negative direction. Given that the oxidation of an PEG unit adsorbed ($[\text{HO}-(\text{CH}_2-\text{CH}_2-\text{O}-)_n\text{CH}_2-\text{CH}_2\text{OH}]_{\text{ads}}$, $n \approx 20$) on the Pt-EQCM surface affords one molecule of the corresponding aldehyde ($[\text{HO}-(\text{CH}_2-\text{CH}_2-\text{O}-)_n\text{CH}_2-\text{CHO}]_{\text{ads}} + 2\text{H}^+$) adsorbed on the Pt-EQCM surface, the change in mass on the electrode surface following the oxidation is very small and is not appreciable in our results.

4.CONCLUSIONS

The present study examined the adsorption of PEG with various molecular weights (400, 3000, 8000, or 20000), and its coadsorption with Cl^- ions through an analysis of quantitative data obtained from simultaneous voltammetric and EQCM measurements.

The results show that in a solution free of Cl^- ions, the PEG_X molecules are adsorbed at the open circuit potential (E_{OCP}). Under these conditions, the adsorption of PEG_X on Pt does not interfere with the oxidation of the surface to create a film of PtO. During the potential scan in the negative direction, three processes involving the partial desorption of PEG_X from the Pt-EQCM electrode surface are observed. At the end of the potential scan in the negative direction, a fraction of the electrode surface remains covered with PEG_X molecules; this fraction increases with increasing molecular weight of PEG_x, reaching a maximum value of 0.217 for PEG₂₀₀₀₀. In addition, the anodic current density in the voltammogram and the mass flux in the massogram in the potential interval 0.5 to 0.80 V increase with increasing PEG_X molecular weight. That is, the increase in current density in this potential interval is accompanied by an increase in the mass adsorbed on the electrode surface. On the basis of these results, we propose that the anodic process observed in the potential interval 0.5 to 0.80 V corresponds to the oxidation of PEG units (formed by the scission of PEG_X in acidic media), including both the PEG units adsorbed on the electrode surface and those in solution. The oxidation of each PEG unit gives rise to one molecules of the corresponding aldehyde, which remain adsorbed on the electrode surface.

We also found that compared to the solutions without Cl^- ions, a larger quantity of PEG_X was adsorbed at E_{OCP} when Cl^- ions were present in the electrolyte solution. In addition, one adsorption process and two partial desorption processes were observed at the surface of the Pt-EQCM electrode during the potential scan in the negative direction. At the end of the Potential scan in the negative

direction, the fraction of the surface covered with PEG units was large as those observed in the presence of molecules PEG_X only. Finally, an interesting result of the present work that has implications for industrial metal electrodeposition processes is that the presence of Cl⁻ ions in the electrolyte solution suppressed the oxidation of PEG_X.

ACKNOWLEDGEMENTS

The authors are grateful for financial assistance provided by CONACyT, projects 48440-Y and 48335-Y. Alia Méndez and L.E. Morón are grateful to CONACyT for scholarship support.

References

1. L. Oniciua and L. Muresan, *J. Appl. Electrochem.* 21 (1991) 565
2. T.C. Franklin, *Plat. Surf. Finish.* 81 (April 1994) 62
3. A. Gomes, M.I. da Silva Pereira, *Electrochim. Acta* 51 (2006) 1342
4. J.J. Kelly, Ch. Tian, A.C. West, *J. Electrochem. Soc.* 146 (1999) 2540
5. F. Lallemand, L. Ricq, P. Bercot, J. Pagetti, *Electrochim. Acta* 47 (2002) 4149
6. G. Trejo, H. Ruiz, R. Ortega, Y. Meas, *J. Appl. Electrochem.* 31 (2001) 685
7. A. Méndez, P. Diaz-Arista, L. Salgado, Y. Meas, G. Trejo, *Int. J. Electrochem. Sci.* 3 (2008) 918
8. J.W. Kim, J.Y. Lee, S.M. Park, *Langmuir* 20 (2004) 459
9. T.Ya. Safanova, D.R. Khairullin, G.A. Tsirlina, O.A. Petrii, S.Yu. Vassiliev, *Electrochim. Acta* 50 (2005) 4752
10. J. Healy, D. Pletcher, M. Goodenough, *J. Electroanal. Chem.* 338 (1992) 155
11. J. Healy, D. Pletcher, M. Goodenough, *J. Electroanal. Chem.* 338 (1992) 167
12. D. Stoychev, I. Vitanova, S. Rashkov, T. Vitanov, *Surf. Technol.* 7 (1978) 427
13. G. Hope, G. Brown, D. Schweinsberg, K. Shimizu, K. Kobayashi, *J. Appl. Electrochem.* 25 (1995) 890
14. J.J. Kelly and A. West, *J. Electrochem. Soc.* 145 (1998) 3472
15. J.J. Kelly and A. West, *J. Electrochem. Soc.* 145 (1998) 3477
16. L. Bonou, M. Ayraud, R. Denoyel, Y. Massiani, *Electrochim. Acta* 47 (2002) 4139
17. M. Petri, D. M. Kolb, U. Memmert, H. Meyer, *J. Electrochem. Soc.* 151 (2) (2004) C793
18. L.E. Moron, Y. Meas, R. Ortega-Borges, J.J. Perez-Bueno, H. Ruiz, G. Trejo, *Int. J. Electrochem. Sci.* 4 (2009) 1735
19. T. Akiyama, S. Kobayashi, J. Ki, T. Ohgai, H. Fukushima, *J. Appl. Electrochem.* 30 (2000) 817
20. J.D. Reid, and A.P. David, *Plat. Surf. Finish.* 74 (January 1987) 66
21. T.Ya. Safanova, N.V. Smirnova, O.A. Petrii, *Russ. J. Electrochem.* 42 (2006) 995
22. R. Woods, in: A.J. Bard (Ed), *Electroanalytical Chemistry*, vol. 9, Marcel Dekker, New York, 1977, p.1
23. S. Langerock and L. Heerman, *J. Electrochem. Soc.* 151 (2004) C155
24. V. Tsionsky, L. Daikhin, E. Giliadi, *J. Electrochem. Soc.* 143 (1996) 2240
25. G. Sauerbrey, *Z. Phys.* 155 (1959) 206
26. K.K. Kanazawa and J.G. Gordon, *Anal. Chim. Acta* 175 (1985) 99
27. M. Urbakh and L. Daikhin, *Langmuir* 10 (1994) 2836, L. Daikhin, M. Urbakh, *Faraday Discuss.* 107 (1997) 27
28. G. Vatankhah, J. Lessard, G. Jerkiewicz, A. Zolfaghari, B.E. Conway, *Electrochim. Acta* 48 (2003) 1619
29. K. Shimazu and H. Kita, *J. Electroanal. Chem.* 341 (1992) 361
30. A. Bewick and J.W. Russell, *J. Electroanal. Chem.* 132 (1982) 337

31. M. Watanabe, H. Uchida, N. Ikeda, *J. Electroanal. Chem.* 380 (1995) 255
32. M.C. Santos, D.W. Miwa, S.A.S. Machado, *Electrochem. Commun.* 2 (2002) 692
33. A. Zolfaghari, B.E. Conway, G. Jerkiewicz, *Electrochim. Acta* 47 (2002) 1173
34. F. Gloguen, J.K. Legar, C. Lamy, *J. Electroanal. Chem.* 467 (1999) 136
35. G. Jerkiewicz, G. Vatankhah, J. Lessard, M.P. Soriaga, Y.S. Park, *Electrochim. Acta* 49 (2004) 1451
36. A. Halperin, M. Tirrel, T.P. Lodge, *Adv. Polym. Sci.*, 100 (1992) 31
37. G.A. Snook, A.M. Bond, S. Fletcher, *J. Electroanal. Chem.* 526 (2002) 1
38. E. Bahena, P.F. Méndez, Y. Meas, R. Ortega, L. Salgado, G. Trejo, *Electrochim. Acta* 49 (2004) 989
39. P. Díaz-Arista, R. Antaño-López, Y. Meas, R. Ortega, E. Chainet, P. Ozil, G. Trejo, *Electrochim. Acta* 51 (2006) 4393
40. G. Trejo, in: M. Nuñez (Ed.) *Electrochemistry New Research*, Nova Science Publishers Inc, New York, 2005, Ch. 2